Towards an IEEE 802.11 Compliant System for Outdoor Vehicular Visible Light Communications

Muhammad Sohaib Amjad *Student Member, IEEE*, Claas Tebruegge *Student Member, IEEE*, Agon Memedi *Student Member, IEEE*, Stephan Kruse *Student Member, IEEE*, Christian Kress *Student Member, IEEE*, J. Christoph Scheytt *Member, IEEE*, and Falko Dressler *Fellow, IEEE*

***Abstract*—As a complementary technology to existing Radio Frequency (RF)-based solutions such as Cellular V2X (C-V2X) and Dedicated Short Range Communication (DSRC), Vehicular VLC (V-VLC) is gaining more attention in the research community as well as in the industry. This paper introduces a complete IEEE 802.11 compliant V-VLC system. The system relies on USRP software defined radios programmed using the GNU Radio framework, a typical car headlight plus a custom driver electronics for the high-power car LEDs (sender), and a photodiode (receiver). Building upon our earlier work, we, for the first time, experimentally explore the communication performance in outdoor scenarios, even in broad daylight, and show that rather simple optical modifications help to reduce the ambient noise to enable long distance visible light communication. Our system also supports OFDM with a variety of Modulation and Coding Schemes (MCS) up to 64-QAM and is fully compliant with IEEE 802.11. We performed an extensive series of experiments to explore the performance of our system, even using higher order MCSs in daylight. Our results demonstrated a high reliability for distances up to 75 m with the presented system, regardless of the time of the day.**

***Index Terms*—Vehicular-Visible Light Communication, Outdoor VLC, IEEE 802.11, Receiver Optics, GNU Radio.**

I. Introduction

Technological advances in solid-state lighting designs have resulted in the production of highly efficient and robust Light Emitting Diodes (LEDs). Besides their increasing popularity for lighting applications, LEDs are being considered for a new type of application, namely Visible Light Communication (VLC) [1]–[3]. VLC is enabled by the fast switching capability of LEDs, which allows the modulation of digital information onto the intensity of the emitted light. Photo-diodes or camera image sensors are used to demodulate the optical signal on the receiving side.

Initial applications of VLC were intended for indoor communication, and with VLC-enabling front-ends becoming commercially available [4], this technology has already been deployed in healthcare facilities, classrooms, etc. Meanwhile, multiple standardization efforts in the scope of IEEE 802 standards family and JEITA have taken place, leading to IEEE 802.15.7 [5] for photodiode based VLC, IEEE 802.15.13 based on Optical Camera Communication (OCC), and IEEE 802.11 LC, which aims to amend base IEEE 802.11 standard and enable communications in the visible light medium.

Recently, LED-based exterior lighting modules are also proliferating in the automotive industry. The energy efficiency of LEDs, which is gaining in importance with the increasing electrification of vehicles; the robustness against vibrations, which yields longer service time; and the small form factor, which allows more versatile design; are some of the advantages that have motivated for the rapid adaptation of LEDs in the automotive industry. In turn, this has opened a new application domain, i.e., Vehicular VLC (V-VLC) [6]–[12].

V-VLC can be considered a low-cost access technology for vehicular networking, since potential VLC transmitters (i.e., LED-based headlights and taillights) are readily available, whereas, the receivers might be present (e.g., rear-view camera), or can be incorporated at low cost (e.g., photodiode) [6]. Traditionally, vehicle headlights and taillights provide proper illumination and signaling for the drivers, to improve safety on roads. However, with the added communication capability the lighting modules can additionally facilitate Vehicle-to-Vehicle (V2V) applications, as long as the communication does not hinder the primary tasks of illumination and signaling.

There are many properties of VLC that can benefit vehicular networking applications [13], [14]. For instance, the Line-of-Sight (LoS) characteristic and directionality of VLC offers extended spatial reusability of the modulation-bandwidth with tractable collision-domain [15], as well as, enhanced security because the physical obstruction of the Line-of-Sight link is easy to notice, and hard to carry out in driving vehicles [16]. On the other hand, the mobility of the vehicular traffic, and the disturbances in the outdoor environment (e.g., ambient light, strong sunlight, bad weather conditions) impose challenges for the communication [17].

Regardless of the outdoor conditions, a V-VLC system is supposed to provide reliable communication. This is particularly important for safety-related applications, which typically have stringent latency and reliability requirements. To meet these requirements under challenging communication conditions, a V-VLC system should have a carefully designed physical layer, especially with respect to the choice of robust and efficient Modulation and Coding Schemes (MCS) [18], [19]. Orthogonal Frequency-Division Multiplexing (OFDM) in this regard, has emerged as a preferable modulation techniques,

Muhammad Sohaib Amjad, Agon Memedi, and Falko Dressler are with the School of Electrical Engineering and Computer Science, TU Berlin, Germany; Claas Tebruegge is with HELLA GmbH & Co. KGaA, Lippstadt, Germany; and Stephan Kruse, Christian Kress, and J. Christoph Scheytt are with the Heinz Nixdof Institute and System and Circuit Technology, Paderborn University, Germany ({amjad,memedi,dressler}@ccs-labs.org, claas.tebruegge@hella.com, {stkruse,kressc,cscheytt}@hni.upb.de).

primarily because of its resilience to narrow band noise, and it has been widely adopted by many standards including IEEE 802.11. The different narrowband modulation techniques such as BPSK, and higher order QAM, in conjunction with OFDM, provide an efficient yet robust physical layer implementation. Besides that, a V-VLC system also needs to have a linear front-end [20], and an appropriate lighting module (e.g., high beam, or low beam) for communications.

In this paper, we extend our previous work [12], where we presented a complete IEEE 802.11 compliant V-VLC transmitter-receiver system built upon Commercial Off-The-Shelf (COTS) components and a Software Defined Radio (SDR)-based implementation using the GNU Radio framework[1] for baseband signal processing. We now address the issues encountered in [12] and conduct extensive outdoor measurements for different ambient light situations including strong sunlight, which allows to perform real-time experiments using off-the-shelf head- and taillights for V-VLC experiments. By means of our SDR implementation, we are able to study a wide range of MCS for OFDM based V-VLC. For realistic scenarios, our extended prototype currently achieves a data rate of 1.35 Mbit/s with $64-$QAM $3/4$ for distances up to 40 m even in bright sunlight. If we trade data rate for distance, our prototype can achieve ranges beyond 75 m with lower order MCS. Additionally, at a fixed smallest practically possible inter-vehicle distance of 5 m, by choosing higher sample rates operating in the low-pass region of the headlight, a maximum data rate of 8.8 Mbit/s is measured. We see our extended prototype as a first step towards the design of more sophisticated hardware and physical layer solutions for outdoor V-VLC.

Our main contributions can be summarized as follows:

- We present a flexible GNU Radio-based IEEE 802.11 compliant implementation for outdoor Vehicular VLC, which utilizes a high-power LED headlight – driven by highly linear driver circuit that couples it with the SDR, and supports communication distances beyond 75 m, even in broad daylight.
- We confirm that limited bandwidth by the low-pass behavior characteristics of COTS devices are the main performance bottlenecks in OFDM-based V-VLC systems, and highlight that minor system adjustments (i.e., introduction of simple optics on the receiving side) can largely improve the system performance.
- We investigate the outdoor performance of our V-VLC system even in bright sunlight and show that the sunlight does have a strong impact on the Photo-Detector (PD) noise floor but it can be eliminated completely with minor modifications.
- We also investigate the impact of optics alignment on the receiver's performance and analyze the impact of daylight on the PD noise floor in both baseband and passband for different design settings.

II. Related Work

Generally speaking, the V-VLC literature can be divided in two major categories, depending on the type of the employed receiver, which can be a PD [9], [17], [19], [21], [22] or a camera image sensor [10], [13]. These two different ways of realizing V-VLC (and VLC, in general), have distinct properties. We rely on a PD, which is rather cheap, and supports higher switching frequencies, thus, higher bandwidth.

One of the main challenges in V-VLC arises from the hardware limitations (e.g., the slow response time of high-power LEDs), and the challenging outdoor conditions (e.g., high mobility, background noise from sunlight and other light sources). Many studies in the literature have addressed these physical layer challenges as follows.

Liu et al. [9] conduct a comprehensive V-VLC study, including empirical measurements and simulations. In their measurements, they investigate the impact of day time and night time noise sources (i.e., sunlight and artificial light sources) on the Packet Delivery Ratio (PDR). Results show that when the sun is not in the Field of View (FoV) of the transmitter, a PDR of 100 % can be achieved for distances below 100 m. Here, using an optical lens helps to reduce the receiver's FoV. On the other hand, when the optical lens is removed, and there is a direct LoS between the receiver and the sun (at sunrise and sunset) the PDR is reduced to 0 % due to saturation of the receiver. For the night time noise investigation, the authors conduct measurements in the lab, using a halogen light and an LED (to emulate an idle V-VLC transmitter). Results show that the unmodulated LED has no impact on the communication performance, but the halogen light can reduce the PDR to 0 % at very short distances. Despite the breadth of the study, the authors do not use a real vehicle exterior lighting module, instead, they use an LED matrix that does not emulate the radiation characteristic of the real automotive lighting module, which in fact has an impact on V-VLC. The system under consideration can achieve 100 kbit/s data rate using On-Off Keying (OOK).

Shen and Tsai [21] for the first time conduct V-VLC measurements in real-world driving scenarios. Instead of OOK, they use OFDM as a multi-carrier modulation scheme to improve the spectral efficiency of V-VLC. The authors limit the number of subcarriers to 16, instead of the typical 64, in order to obtain better Signal-to-Noise Ratio (SNR) for each subcarrier. Generally, OFDM does not only improve spectral efficiency but also adds good robustness against narrow-band noise that is typically caused by interfering light sources. To achieve the targeted communication distance of 45 m using the taillight, the authors use an optical lens to improve the SNR. In post-processing, the authors report a 70 % symbol reception rate for the targeted distance.

In a follow-up study, Béchadergue et al. [22] compare the performance of OOK modulation to the OFDM system presented in [21]. Results show that OOK achieves comparable performance to OFDM in terms of PDR. However, OFDM is shown to be more resilient to interference caused by LED signs in the traffic. The presented prototype is able to achieve a data rate of 2 kbit/s using OFDM and 100 kbit/s using OOK. The authors demonstrate error-free communication over 60 m, at the expense of reduced data rate due to the used Repetition Coding (RC).

Narmanlioglu et al. [19] use multiple OFDM modulated

[1]www.gnuradio.org

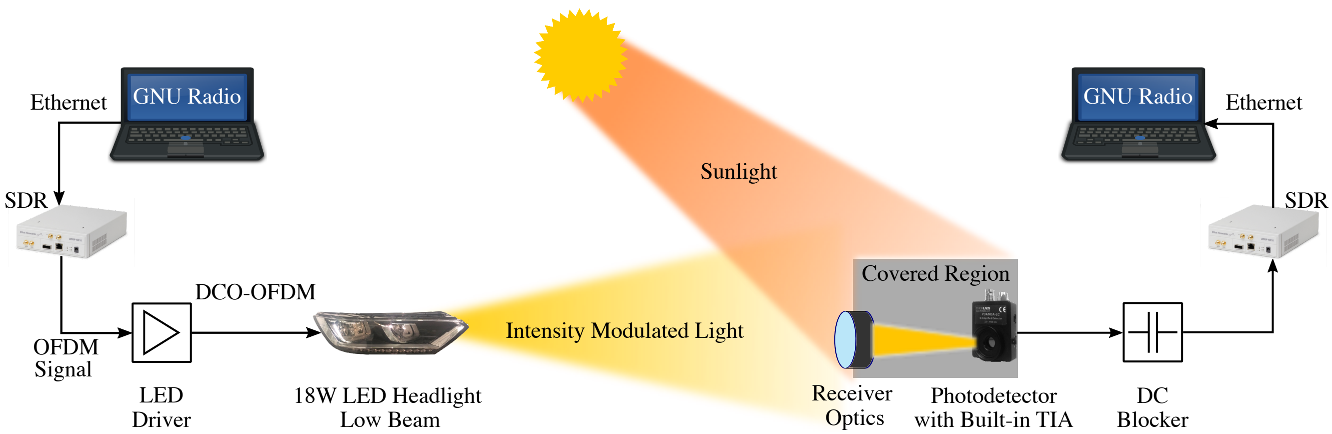

Figure 1. A high-level description of our extended Vehicular VLC transmitter-receiver system for outdoor measurements.

taillights for direct and multi-hop V-VLC. Direct Current-Biased Optical OFDM (DCO-OFDM) is used to modulate the signal which is transmitted via four different taillight combinations, whereas RC and Spatial Multiplexing (SM) techniques are used to realize Multiple-Input Multiple-Output (MIMO). Bit Error Ratio (BER) evaluation reveals that SM MIMO should be chosen over RC because it has better spectral efficiency and achieves the same throughput with lower order modulation. Best BER performance is achieved when only the taillights closest to the PD are used for transmission, and the third brake light (centrally high mounted light) is not used. As the use of the third light results in power division and, therefore, reduced transmission power on all transmitters.

Turan et al. [17] do time and frequency domain characterization of the V-VLC channel, conducting experiments in a static outdoor scenario during different times of the day. In order to account for the effects of background lighting noise on the channel, they do not utilize an optical filter in their setup. In turn, this allows the saturation of the PD when exposed to direct sunlight. Their results show that the sunlight not only impacts the system's effective usable bandwidth, but also reduces the channel gain, compared to sunset and night time measurements.

In our previous works, we presented a highly linear VLC modulator circuit with a bandwidth of 20 MHz, which can be used to realize DCO-OFDM [20]. Additionally, we introduced a GNU Radio-based V-VLC implementation [12], which we used to investigate in detail the performance of different OFDM MCS. Based on extensive measurements in an indoor parking lot, we showed that our system could achieve reliable communication with data rates between 0.15 Mbit/s–0.9 Mbit/s for realistic inter-vehicle distances. Detailed BER investigation of the system was performed in an indoor lab setup with long-term measurements in [18].

This paper extends our basic prototype [12], which is now capable of fully perform in the outdoors, even in bright daylight. Our novel implementation is built upon open-source framework, can be studied in detail considering all aspects, and offers a flexible platform supporting easy modifications for future rapid prototyping. Moreover, it can provide interoperability with IEEE 802.11 devices, and it is in line with the goals of the upcoming IEEE 802.11 Light Communication (LC) standard.

III. V-VLC System Design & Implementation

Our extended V-VLC prototype design for outdoor communications is depicted in Figure 1. The prototype design comprises of two parts: First, the digital signal processing part, which is using laptop PCs running GNU Radio and SDRs (e.g., two N210 Universal Software Radio Peripheral (USRP) from Ettus Research); and, secondly, the VLC enabling front-ends that includes a VLC driver circuit (which is available as open hardware[2]), a headlight, some receiver optics, and a photodetector with DC blocker.

A. Baseband Signal Processing

In our VLC system, the baseband signal processing is done in the GNU Radio framework. In related work, also Field-Programmable Gate Arrays (FPGA)-based SDRs such as the WARP Mango board are used, which offer deterministic timing and low latency. However, they are rather inflexible and it is often challenging to implement complex signal processing algorithms. In contrast, the GNU Radio framework is General Purpose Processor (GPP)-based, which is not only easily accessible but also supports signal processing using high-level programming languages C++ and Python, thus, making it particularly easy to use, modify, and debug.

For the baseband transmitter/receiver implementation, we modified the GNU Radio-based Open Source stack for IEEE 802.11a/g/p developed by Bloessl et al. [23]. The core of this framework is a modular OFDM transceiver that is fully interoperable with commercially available systems and has been thoroughly evaluated in [24]. The main motivation for building upon this implementation is to test and evaluate the performance of our V-VLC system with commercially available prototypes, as soon as these become available.

Figure 2 illustrates the detailed block diagram of the GNU Radio-based IEEE 802.11 compliant OFDM transmitter and receiver modules. The transmitter implementation is rather

[2] https://www.hni.uni-paderborn.de/sct/projekte/vlc-projekt/

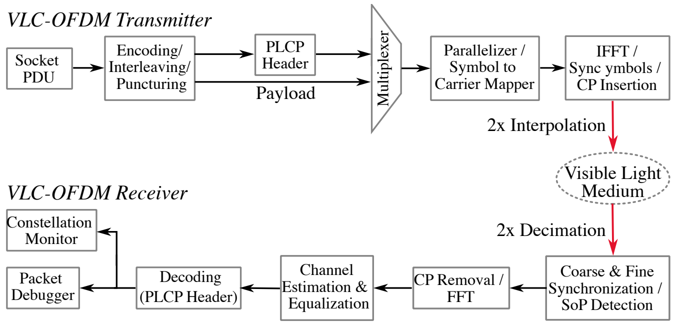

Figure 2. Detailed baseband level block diagram of the OFDM implementation in GNU Radio.

straightforward as the signal is fully specified in the IEEE 802.11 standard. Additionally, a 2x interpolation filter is employed on the raw OFDM samples to further improve the spectral image and shape of the transmitted signal. The transmitter supports all packet sizes and IEEE 802.11 compliant MCS as listed in Table I.

In contrast, the receiver implementation is a design decision and it is generally a trade-off between complexity and performance. The most crucial stages in the receiver design include frame detection/synchronization and channel estimation/equalization. The receiver implementation in our VLC system supports the four channel estimation techniques listed in Table I. In previous work [18], we have already evaluated their performances and found Least Square (LS) being the best estimator in terms of both performance and complexity.

We have used N210 USRP SDRs equipped with LFTX/LFRX daughterboards in our measurements. These specific daughterboards support an operational-bandwidth ranging from 0 MHz–30 MHz, which is well suited for VLC. The baseband OFDM samples from GNU Radio are fed to the transmitting SDR through an Ethernet port. The SDR converts these samples into an analog signal and up-converts the resulting baseband signal to a carrier frequency. The reason for this up-conversion is to overcome the ambient noise that exists in the low frequencies, and can then be easily filtered at the receiver through a high-pass filter. It is important to mention here that the resulting output of the SDR is a bipolar signal preserving all the IEEE 802.11 adaptations.

B. VLC Front-Ends

In contrast to RF communication, where a modulated voltage signal is converted into electromagnetic radiation by an antenna, in VLC with Intensity Modulation and Direct Detection (IM/DD), the modulated signal is converted into a corresponding optical power by using LEDs. It is possible to carry out the modulation in the baseband, but to avoid flickering and to achieve robustness against interference from other light sources, a carrier frequency of 2.3 MHz was chosen for the electrical signal. Alternatively a more complex receiving optics could be used to suppress interference and thus provide a larger usable bandwidth [25]. Since the light intensity is exclusively positive, only unipolar signals can be transmitted. The conversion of bipolar signals of the SDR to a unipolar current signal is done in hardware by the driver. This driver contains a bias tee which creates an offset, whereby the signal is shifted into the positive range. By selecting the bias current the brightness can be easily adjusted. For this experiment, as in [20], a bias current of 300 mA was selected in order to achieve the highest possible linear range, which corresponds to a dimming of about 50 %. Likewise, at the receiver, the Intensity Modulation (IM) light signal is detected by means of photosensitive devices such as camera image sensors or photodiodes. The receiver is followed by a Direct Current (DC)-blocker that renders the DCO-OFDM to an ordinary bipolar OFDM signal, which is then mixed down and processed in the baseband (via SDR) for data retrieval.

The existing LED-based headlights are solely designed to illuminate the street. Since communication is not the intended goal, naturally, the switching speed of the LEDs (that rather defines the bandwidth of a VLC system) has never been a major concern. Consequently, the available headlights have a small operational-bandwidth. This bottleneck has been compensated to some extent through efficient spectral usage, i.e., improved bit/s/Hz, which our OFDM implementation essentially provides by supporting 8 different MCS based on the received SNR.

1) Headlight Driver Circuit: The transmitting SDR produces a voltage signal for the payload to be sent. However, the luminous flux of the headlamp LEDs is nearly linear to the current in a given range. Therefore, a linear Transconductance Amplifier (TCA) is first required to convert the voltage signal into the current. Additionally, with modulation schemes such as OFDM, high Peak-to-Average Power Ratios (PAPRs) is an inherent issue which only gets worse with higher-order MCS. Thus, to support higher-order MCS in the V-VLC prototype, the headlight driving circuitry is required to be linear for a wide range of input signal. Furthermore, an appropriate biasing is also critical for the optimal functionality of the LEDs, otherwise, some parts of the input signal may experience clipping, which might cause distortion, and consequently, performance losses. Hence, a driving circuitry that effectively combines an AC signal current-path with an adjustable DC current biasing is required. In our previous work [20], a highly linear driver circuit with the capacity to efficiently drive the COTS headlight is proposed. The driver circuit shown in Figure 3a includes an internal bias tee which provides a DC bias (I_{DC}) to the AC current signal ($i_{\mathrm{AC}}(t)$) within the linear region of the LEDs. The bias current and the amplitude is adjusted to operate in the largest possible linear range in [20], resulting in a Total Harmonic Distortion (THD) of less than

Table I
KEY PHYSICAL LAYER PARAMETERS OF THE GNU RADIO OFDM IMPLEMENTATION.

Modulations	BPSK, QPSK, 16-QAM & 64-QAM
Code rates	1/2, 3/4, 2/3
Channel equalization	LS, LMS, STA, Linear Combiner
Interpolation factor	2x
FFT/IFFT size	64 points
PLCP (preamble + header)	(4 + 1) OFDM symbols

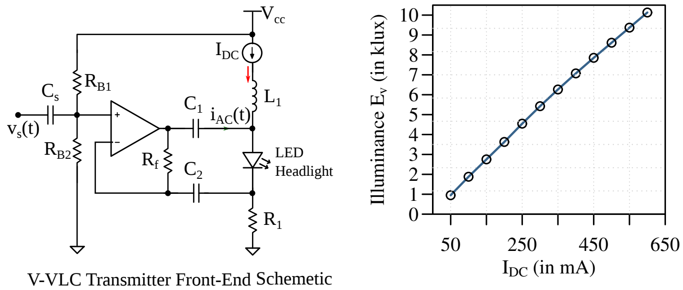

(a) Headlight driver circuitry (b) Illuminance vs. DC current

Figure 3. Headlight driver circuitry and transmission chain linearity [20].

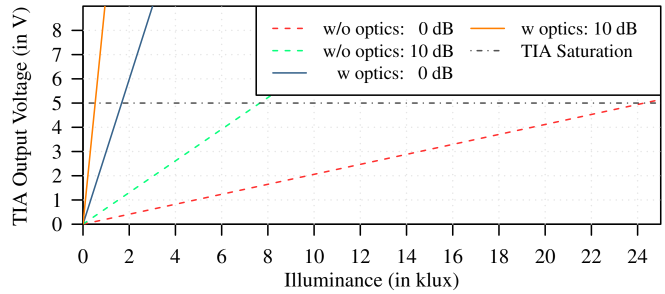

Figure 5. Impact of incident light saturating the used PDA100A-EC Photo-Detector with and without the optics.

5% – over the whole input range. As shown in Figure 3b, the current-to-illuminance ratio already provides a large linear range.

2) Photo-Detector: We have used PDA100A-EC Photo-Detector developed by Thorlabs (with a built-in variable gain amplifier) for the detection of incident IM light signal from the headlight. Inside the PD, the photodiode first converts the incident light to photo-current, and then transform it into a voltage signal via the linear Transimpedance Amplifier (TIA) incorporated within the PD. The resulting voltage signal is forwarded to the SDR for further baseband signal processing via GNU Radio, where the transmitted payload is retrieved.

3) Receiver Optics: The used Photo-Detector already has a large aperture area that offers high sensitivity. To further converge the intensity-modulated light at the PD's aperture, we have introduced a simple optics in our V-VLC prototype. The utilized optic design includes two biconvex lenses with adjustable distance for fine-tuning the focal length as illustrated in Figure 4. The optics is placed in front of the PD to focus the (collected) incident light onto the aperture of the PD. The achievable gain through the used optics (G_{optic}) can be computed as

$$G_{optic} = \frac{\Phi_{\text{ep}}}{\Phi_{\text{PD}}} = \frac{A_{\text{ep}}}{A_{\text{PD}}} = \frac{\pi \frac{d_{\text{ep}}^2}{4}}{d_{\text{PD}}^2}, \quad (1)$$

where Φ_{ep} and Φ_{PD} are the incident radiant fluxes at the entrance pupil and at the photo-detector (without any optics), respectively, A_{ep} and A_{PD} are the entrance pupil areas; which in this design are the areas of the first lens and the PD, and d_{ep} and d_{PD} are the diameters of the first lens and the PD aperture, respectively. With an area of $100\,\text{mm}^2$ of the used PD and an area of $1452\,\text{mm}^2$ of the first lens, the acquired optical gain is close to 11.6 dB. It is important to mention here that the optic design placement in the V-VLC prototype is specific for this experiment scenario only. For on the road applications, the FoV may need to be changed by a factor of focal length.

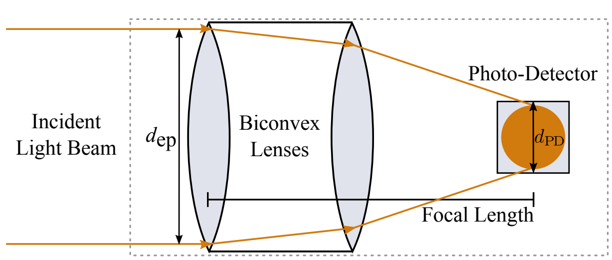

Figure 4. Schematic explaining the receiver optics.

IV. Design Modification for V-VLC Operation in Bright Daylight

To enable reliable communication in outdoor environments, e.g., in the presence of bright sunlight, we had to modify our previous design. The intensity of the sunlight is generally high, but constant (or the changes are very slowly compared to the intensity-modulated signal), so that it can be filtered by a high pass filter. Nevertheless, based on our experimental observations, the situations in which the strong sunlight directly hits the PD result in the saturation of the PD. Figure 5 demonstrates the saturation behavior of the used PDA100A-EC PD, when the light is directly incident on the PD aperture. Even in the simplest case of no optics and without any TIA gain, the maximum illuminance the PD can handle is 24 klux. The introduction of optics can further focus the directly incident light on the PD aperture, which reduces the input illuminance capacity of the PD below 2 klux. This saturation of TIA, however, only happens when the light is directly incident on the PD aperture. In such situations, it is impossible to receive the desired intensity-modulated signal from the headlight and therefore communication is not possible.

We addresses this PD saturation problem in two steps: First, the FoV is optimized. It should be noted that the selection of the FOV is usually a trade-off between noise reduction and the possible angle of reception. With adaptive receiver optics, however, a high noise reduction with a large reception angle is possible [25]. We further cover the entire path in the optic design, i.e., between lens and PD, to block the light from unwanted angles as illustrated in Figure 1. Secondly, the strong DC-component is blocked at an earlier stage by placing the DC-blocker before the USRP. For use at night time, these modifications are not really necessary, and, theoretically, the unmodified design can be used. Nevertheless, for a fair comparison, we did not alter the design during our measurement campaign.

To further study the impact of sunlight on the optical receiver's performance, we conducted a series of noise measurements in broad daylight. For clarity, we present only selected, most relevant measurements. We measured the noise values at both baseband and passband levels (cf. Figure 6).

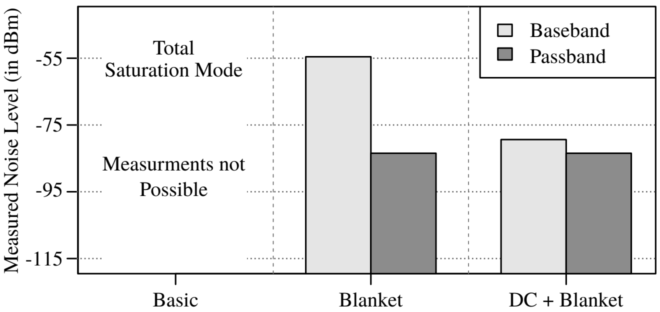

Figure 6. Impact of our different design modifications on the receiver's noise levels in broad daylight.

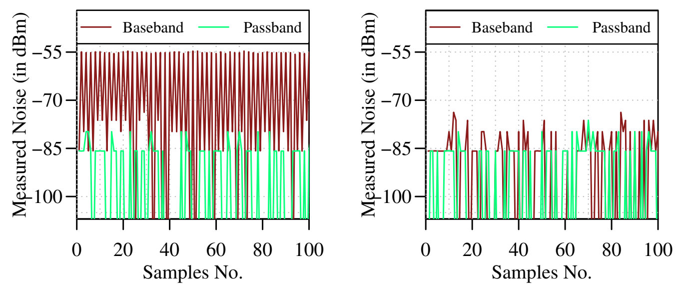

(a) With blanket only (b) With blanket and DC blocker

Figure 7. Received samples at baseband and passband levels in broad daylight.

The first measurement setting with the basic setup is based on our previous design (see [12]), without the covered region and DC blocker. As expected, the strong daylight in this setup, led to the total saturation of the PD and appeared to be useless for outdoor measurement during the day time.

In the second setting, we covered the region between the lens and PD (as illustrated in Figure 1) with a thick blanket to block the direct daylight. As compared to the basic setup (with total saturation), the USRP was able to record the samples. The averaged noise measured in both baseband and passband stages is presented in Figure 6, where the noise in the baseband is approximately 30 dB higher than in the passband. Additionally, the received baseband and passband noise samples are shown in Figure 7a. It can be seen that the passband noise is merely the quantization noise due to the Analog-to-Digital Converter (ADC) in the received signal processing path, whereas the baseband noise (due to sunlight) is somewhat periodic and much stronger close to −55 dBm.

The third setup, which completes our extended prototype (cf. Figure 1), further includes a DC blocker following the PD. From Figure 6 it can be seen that the baseband noise is significantly reduced by the addition of DC blocker in the receiving path. Nevertheless, it is still approx. 5 dB higher compared to passband noise. Figure 7b shows the noise samples received in the third setting, where the baseband noise with the addition of DC blocker is now close to the quantization noise of the ADC. Since the main noise factor is introduced by the electronic components rather than the (ambient) light, we decided not to spend further efforts to measure the exact noise (shot and thermal noise of the PD). Some first analytical quantifications of these noise components have already been presented in the literature [25].

These results help to characterize the behavior of sunlight as close to DC, i.e., resides in the baseband, and that it can be significantly reduced through a simple DC blocker. Additionally, the identified baseband noise behavior evidently supports the idea of up-conversion of the desired signal before intensity modulation, as it basically bypasses the interference from low-frequency ambient noise sources that maintain a higher noise level in the baseband. In conclusion, the impact of sunlight as substantial it may sound at the first guess, is not that severe in reality, and can be addressed with rather simple design modifications.

V. Experimental Evaluation

In this section, we report selected results from a measurement campaign using our system, focusing on an outdoor scenario. As a baseline, we first calculate the expected Received Signal Strength (RSS) over distance for the used headlight analytically, and then present real-world experimental results.

A. *Analytical Baseline*

Since the performance of V-VLC essentially depends on the RSS of the LoS path, an analytical calculation of the signal strength over the distance has been performed to obtain baseline RSS values. The RSS analytics is based on the beam characteristic of the headlight used, which contains the luminous intensity for each radiation angle, and it is essentially obtained by integrating the illuminance over the area of receiving pupil, taking into account the spectrum of the LED and the sensitivity of the photodiode. The analytical computations are carried as follows.

First, the luminous flux $\Phi_{V,\Omega}$ is calculated by the integration of the luminous intenisty, $I_V(\alpha_h, \alpha_v)$, over the solid angle, Ω, projected on the area of the entrance pupil as

$$\Phi_{V,\Omega} = \iint_{\Omega} I_V(\alpha_h, \alpha_v)\, d\Omega, \tag{2}$$

where Ω is obtained from the entrance pupil of the receiver optics A_{ep} [26], and the receiver's distance r as [27]

$$\Omega = \frac{A_{ep}}{r^2}. \tag{3}$$

Here, the position of the receiver is defined by the distance r, and the horizontal and vertical angles (α_h, α_v) that are included in the radiation pattern of the headlight, i.e., the luminous intensity function $I_V(\alpha_h, \alpha_v)$.

The photocurrent, I_{PD}, of the PD can then be calculated using the luminous flux, $\Phi_{V,\Omega}$ as

$$I_{PD} = \frac{\int_0^\infty d\Phi_{V,\Omega}(\lambda) \cdot \mathcal{R}(\lambda)\, d\lambda}{\int_0^\infty K_m \cdot V(\lambda)\, d\lambda} \; . \tag{4}$$

Here, the product of the spectral density function of the luminous flux, $d\Phi_{V,\Omega}(\lambda)$, and the sensitivity of the diode, $\mathcal{R}(\lambda)$, is integrated over the wavelength, λ, to take into account the sensitivity of the PD towards the radiated light. This product is divided by the integrated product of the sensitivity of the human eye, $V(\lambda)$, and maximum value of the photometric radiation equivalent, K_m, over the wavelength, λ, to remove the sensitivity of the eye from the luminous flux.

Figure 8. Measurement facility, and the transmitter-receiver setup.

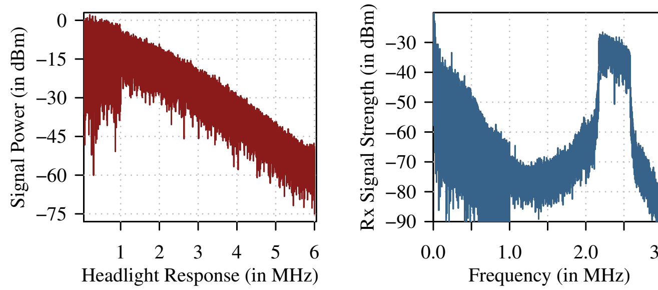

(a) Headlight frequency response (b) Detected OFDM signal

Figure 9. Impact of low-pass behavior of the headlight on the transmitted OFDM signal.

The power at the PD, P_{PD}, is finally computed by taking into account the amplification of the TIA, G_{TIA}, and the terminating resistor

$$P_{PD} = \frac{V_{\text{PD}}^2}{50\ [\text{Ohms}]} = \frac{(I_{\text{PD}} \cdot G_{\text{TIA}})^2}{50\ [\text{Ohms}]}. \quad (5)$$

For good comparability, the same parameters are used for the analytical calculation of the signal strength as in the outdoor experiments (cf. Table II). This includes the exact headlight type (for this study a VW Passat 18 W LED-based low beam headlight), the height difference, the PD with the corresponding sensitivity curve, the optics gain, and the TIA gain of 10 dB. An investigation of the analytical as well as the experimentally measured RSS is carried out in Section V-C together with Figure 13.

B. Measurement Setup

For the performance analysis of our outdoor V-VLC system, we conducted live-measurements in an open-air car parking facility. Figure 8 shows our experimental setup in the measurement facility. The chosen location for the measurements provides adequate space with reasonably long transmitter-to-receiver separation distances without interruption. Furthermore, this outdoor facility enables the study of adverse time-varying characteristics of the sunlight, thus, allowing us to evaluate the system's performance under bright sun as well as at night. As a baseline, an analytical model for the RSS is additionally used.

To evaluate our V-VLC prototype experimentally, we performed extensive measurements in the described outdoor facility. In the measurement campaign, we positioned the headlight along with the driving circuitry and other transmission chain hardware on one end of the parking facility. We fixed the PD and corresponding receiving chain hardware on a mobile cart, and then in a straight line, increased the distance between the transmitter and receiver incrementally. The 2.5 m equidistant marks on the parking lot ground, assisted in the cart stationing at incremental distances for even measurements.

For each MCS listed in Table I, we transmitted 1000 OFDM packets of size 250 B (2×10^6 bit per transmission) at every measurement point, and obtained the PDR and the RSS values at the receiver. The TIA gain (within the PD) is also varied from 0 dB–70 dB during different measurement campaigns. Additionally, approx. 11.6 dB optical gain is obtained exclusively through the receiver optics. A maximum separation distance of 75 m between the transmitter and receiver is only possible due to the space constraints of the facility.

Table II summarizes the most important parameters of our measurement campaign.

1) Frequency Response and Achievable Data Rates: We have up-converted our baseband signal to a center frequency of 2.3 MHz. While this translation to a higher frequency attenuates our baseband signal by a reasonable factor because of the LEDs low-pass behavior, this makes our system robust against ambient noise sources. Figure 9a demonstrates the low-pass behavior of the used headlight, where on average, the signal strength is reduced by 10 dB per 1 MHz. This is consistent with the measurements of the high-power LEDs in [17]. For a sampling frequency of 1 MHz and a 2x interpolation rate, the resulting OFDM signal is shown in Figure 9b, where it can be seen that the power difference between lowest and highest sub-carrier frequency is 5 dB. With this bandwidth of 500 kHz, our system achieves a maximum data rate of 1.35 Mbit/s reliably up to 40 m. Compared to the ones reported in the literature for typical indoor VLC [28], the achieved data rates can be considered relatively low. However, this is only due to the slow switching frequency of the high brightness LEDs used in an average design of automotive lighting modules, which

Table II
HARDWARE SPECIFIC PARAMETERS FOR THE MEASUREMENTS.

Headlight	VW Passat 18 W LED-based low beam
Headlight's 3 dB bandwidth	1.3 MHz
PD	Thorlabs PDA100A
PD's 3 dB bandwidth	2.4 MHz
PD gain	0 dB–70 dB
Relative height RX/TX	63 cm
Distance between RX/TX	2.4 m–75 m
Optics gain (G_{optic})	11.6 dB
Center frequency	2.3 MHz
Sampling frequency	1 MHz
Data rates	0.15 Mbit/s–1.35 Mbit/s

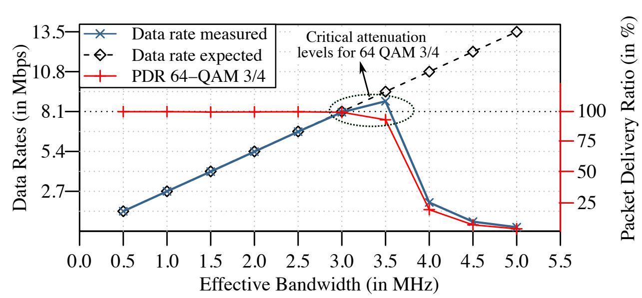

Figure 10. Measured data rates together with the PDR at smallest practically possible distance of 5 m with increasing sample rates.

restricted us to use lower sampling frequency, i.e., 1 MHz. Note that higher sampling rates can also be utilized to achieve better data rates at shorter distances, where the high received SNR can be used to compensate for the headlight's low-pass behavior.

To further investigate the maximum achievable data rates, we considered the smallest practically possible inter-vehicle distance of 5 m between Tx (headlight) – Rx (PD), and increase the sample rates from 1 Msps–10 Msps providing an effective bandwidth of 0.5 MHz–5 MHz. The resulting data rates are shown in Figure 10. In the plot, it can be seen that for bandwidths higher than 3 MHz the PDR starts to drop rapidly, and so does the measured data rate. The curve starts to deviate from the expected maximum data rate, and drops sharply after 3.5 MHz bandwidth. Although the data rate increases from 8.1 Mbit/s–8.8 Mbit/s in the range between 3 MHz–3.5 MHz bandwidth, it is still lower than the expected data rate of 9.45 Mbit/s This is because the received SNR reaches critical levels for bandwidths over 3 MHz–3.5 MHz due to the headlight low-pass behavior, particularly affecting the higher OFDM carriers. Therefore, the system needs to opt for lower order MCS, i.e., QPSK and BPSK, in order to maintain 100 % PDR at higher bandwidths, and none of these modulation schemes can beat the maximum achieved 8.8 Mbit/s data rate, even with a bandwidth as high as 5 MHz. The measured data rates and PDR results in Figure 10 are in line with the headlight frequency response presented in Figure 9, with RSS dropping 10 dB per 1 MHz, and suggest the maximum usable bandwidth of 3 MHz–3.5 MHz at the smallest practically possible inter-vehicle distance of 5 m.

2) Clocking Offset: In our previous work [12], we demonstrated the impact of the drift between transmitter and receiver clocks, resulting in a periodic sampling frequency offset. This clocking offset caused periodic distortion in the received constellation, which appeared to be more severe in higher-order MCS, where the constellation points have smaller Euclidean distance, and thus making symbol decoding decisions more error-prone. A 64-QAM MCS with unsynchronized internal clocks of the SDRs, experimentally demonstrated a per-packet BER of around 50 % over periodic intervals (depicted in Figure 11), due to the clock drift causing periodic sampling offset. Additionally, there were no periodic error bursts recorded when a common external clock for both transmitter and receiver was used. Therefore, in this work, to avoid this burst error behavior, we employed an external clock source. We used two 40 m long coaxial cables to ensure clock synchronization between transmitter and receiver. With external synchronization, we are able to measure the optimal performance of our extended V-VLC prototype for outdoor scenarios, even with higher-order MCS. Nevertheless, with a complete Vehicular VLC system, the problem of clock-frequency synchronization can be potentially addressed efficiently through GPS systems.

3) Illuminance Levels: Figure 12 illustrates the amount of illuminance recorded, and the corresponding noise levels, during the measurement campaign at different times of the day. These measurements have been carried out in a summer day, with back-and-forth changes in the sky conditions, i.e., from bright sunny to partly cloudy and vice versa. In the case of strong and direct sunlight hitting the lux meter, the highest luminance recorded was around 100 klux, whereas during the deepest night hours the luminance value dropped down to 5 lux. For accurate illuminance measurement, the lux meter was always placed in parallel to the photo-detector, such that the incident light is same on both. The day time measurements were conducted in the afternoon from 15:30 to 16:30, with ambient illuminance fluctuating between 6 klux–10 klux (cf. Figure 12). The night time measurements have been performed after 21:00 in the presence of only dim streetlights with illuminance values below 15 lux, which is roughly one-thousandth of the illuminance during day time. The most interesting finding in the plot is that the noise measured against each luminance level is roughly similar (below −84 dBm) regardless of the time of the day, which clearly indicates the resilience of our system towards ambient light.

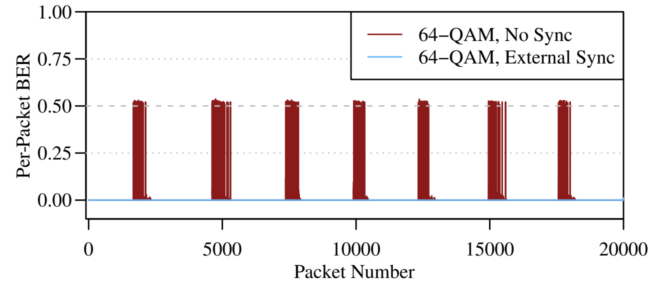

Figure 11. Impact of unsynchronized and externally synchronized clocks of the used SDRs on the BER of VLC receiver in a controlled lab setup.

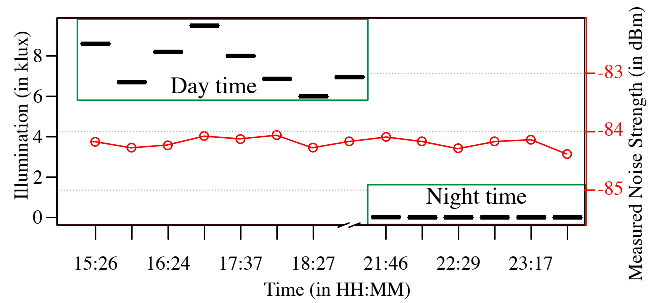

Figure 12. Illuminance levels and the corresponding noise strength measured during different times of the measurement campaign in our outdoor setup.

C. Received Signal Strength over Distance

In Figure 13, analytically obtained RSS and the experimentally obtained signal and noise strengths at the receiver are plotted for increasing distance with our extended prototype. These measurements were obtained with a fixed 10 dB internal gain of the PD. It is important to mention here that without the modifications proposed for the outdoor prototype, the receiving PD remains in total saturation mode and detects nothing, as discussed in Section IV. For the prototype performance without the modifications in indoor/night time measurements see [12]. The prime sources of noise in the VLC systems are the shot noise that is introduced by the PN-junctions of diodes, the interference noise by ambient light, the quantization noise due to ADCs, and the thermal noise produced by electrical

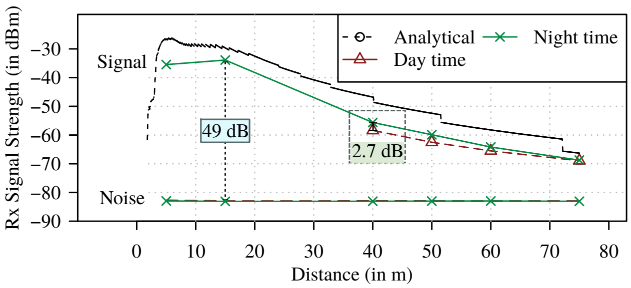

Figure 13. Experimentally measured and analytically calculated RSS and noise levels at both day and night times in our outdoor setup.

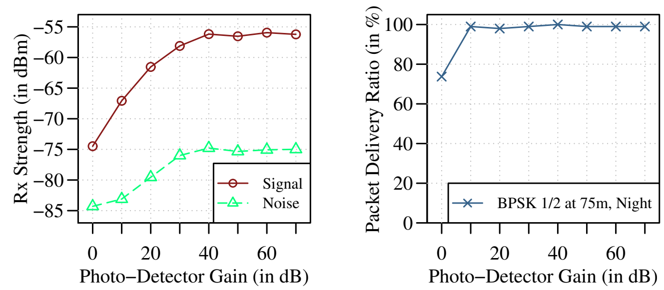

(a) PD gain vs receiver sensitivity. (b) PDR with increasing PD gain.

Figure 14. Impact of TIA gain within the PD, on the overall performance.

components. In the figure, it can be seen that the noise power at every measurement point in our experimental scenario remains below −84 dBm (almost constant), regardless of the distance and time of the day. This similar noise behavior in the passband at both day and night times is also in line with our initial noise measurement (Section IV) in bright daylight and clearly demonstrates the close to negligible impact of the sun on noise levels during the day time.

The received signal strength, on the other hand, first improves with growing distance (i.e., up to 15 m), and then degrades rapidly with further increasing distances. The initial increase in the signal strength is because of the optimal FoV of the PD at a certain distance. This optimal FoV point highly depends upon the relative height of headlight and PD. This rapid signal attenuation is essentially due to the heterogeneous distribution of light which results in strong spatial dependency [11], the inverse square law, and the propagation medium, e.g., the particles presence in the air. Additionally, these experimental results are also in line with the baseline RSS values obtained analytically, and demonstrate a similar RSS behavior. These baseline values can be seen as the upper bound for RSS with the given hardware and a pure LoS connection, since they consider the highest possible amplitude. Due to the increased number of measurement points, the analytical observation shows a rather detailed course of the RSS over the distance. Additionally, the RSS obtained analytically initially increases from a small value over distance. This can be explained by the fact that the receiver is at low vertical angles relative to the transmitter due to the difference in height and that headlights typically emit little light in this direction. At a distance of about 5 m the maximum RSS is reached; afterwards, it decreases monotonously. The degradation in the RSS is mainly due to the inverse-square law. Also, the small steps in the curve are caused by the resolution of 0.2° for the radiation pattern of the headlight.

It is worth noticing in Figure 13 that the RSS during day time is 2.7 dB lower than at night time (at 40 m), and the RSS difference reduces with distance. This reduced RSS could be due to the measurement errors such as (i) misalignment in the optics design, (ii) misalignment of the cart carrying the receiver setup, and (iii) headlight displacement, while measuring at different times of the day. Additionally, this RSS difference could also be because of some other natural variable, e.g., the amount of particles in the air. Moreover, with a higher level of ambient light (during day time), the operation point of the PD certainly changes, which could result in a lower RSS as well. In any case, to accurately model the error cause, substantially more measurements are required over multiple days with a multitude of iterations. Regardless, this difference is relatively small, and cannot overshadow the interesting findings for outdoor V-VLC.

D. Impact of Transimpedance Amplifier Gain

Figure 14a shows the impact of the PD gain on the received signal and noise powers. The Thorlabs PDA100A photodetector used in our V-VLC prototype has a 3 dB-bandwidth of 2.4 MHz that reduces down to approx. half with every 10 dB increase in gain.[3] Due to this reason, the relation between RSS is not linear with PD gain, and after 40 dB gain the 3 dB bandwidth is reduced down to 225 kHz, which is significantly small compared to the used bandwidth already up-converted at 2.3 MHz to combat the ambient effects in the measurement campaign. As a result, any further increment in the gain does not improve the RSS at all. Nevertheless, the figure does provide some valuable insights and specifies that up to 40 dB of PD gain can be used to provide maximum RSS of −56 dBm at 75 m distance. Additionally, Figure 14b shows the corresponding PDR with BPSK 1/2 at 75 m distance for incremental gain in night hours. These results certainly indicate that with higher gain values (e.g., 40 dB) 100 % PDR can be achieved even for further distances.

E. Packet Delivery Ratio over Distance

Figure 15 demonstrates the PDR measured with each MCS for the increasing distance between the VLC transmitter and receiver during the day and night times, respectively. In the plot, the horizontal dashed line marks 90 % PDR, and a 100 % PDR means that all packets have been precisely detected and decoded. Also, these PDRs are obtained with a fixed 10 dB gain of the PD. We measured 100 % PDR to the very end of the measurement facility, i.e., a distance of 75 m, for lower order MCS (BPSK and QPSK) as well as for 16−QAM 1/2 during both day and night times. In-comparison to the experimental results presented in the V-VLC literature [29], such a high PDR performance over 75 m distance in the outdoor setup is

[3] https://www.thorlabs.de/thorproduct.cfm?partnumber=PDA100A

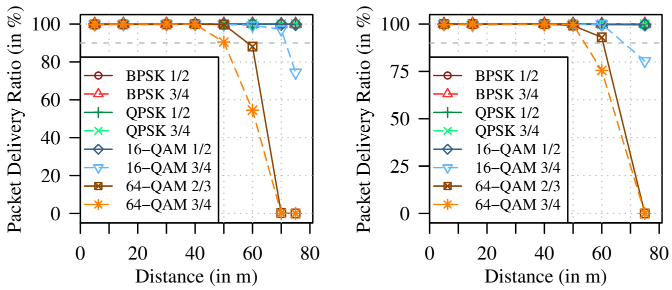

(a) PDR during day time. (b) PDR during night time.

Figure 15. PDR performance for every MCS obtained experimentally for 1000 packets sent per transmission.

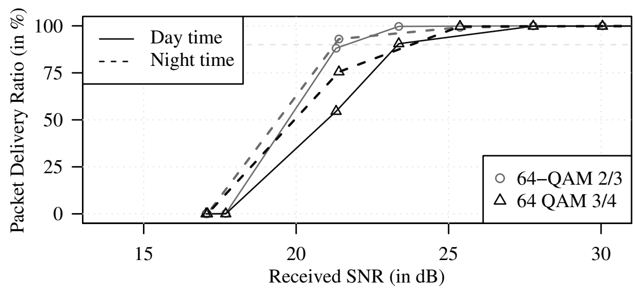

Figure 16. PDR performance of 64−QAM at two different times of the day against received SNR for 1000 packets sent per transmission.

truly remarkable. Even 16-QAM 3/4 is offering an even–close to 90 %, PDR performance at a distance of approx. 70 m.

Additionally, the external clock synchronization has eliminated the irregular drops in PDR with 64-QAM (such as in our previous work [12]), and now, even with 64-QAM 3/4, a PDR of over 90 % is recorded at distances of 50 m and 55 m at day and night times, respectively. The slightly low PDR performance during day time is certainly because of the relatively lower RSS values measured during this time – we already discussed the reasons in Section V-C.

F. Packet Delivery Ratio over Received SNR

Figure 16 shows the PDR performances of 64−QAM 3/4 and 64−QAM 2/3 against received SNR levels. In the plot, the horizontal dashed line marks 90 % PDR threshold, and a 100 % PDR means that all packets have been precisely detected and decoded. It can be seen that both MCS achieved 100 % PDR roughly at similar SNR levels regardless of the time of the day and illuminance intensity. For 64−QAM 3/4, the SNR required is approx. 26 dB, and for 64−QAM 2/3, the SNR requirement is roughly 25 dB. The small deviation in the measured SNR values at two different times of the day is certainly due to measurement errors, which resulted in different RSS, as already discussed in Section V-C. These obtained results not only help in the evaluation of the communication schemes in terms of minimum SNR requirements, but they clearly assert our findings with the presented V-VLC implementation, even in a realistic outdoor scenario.

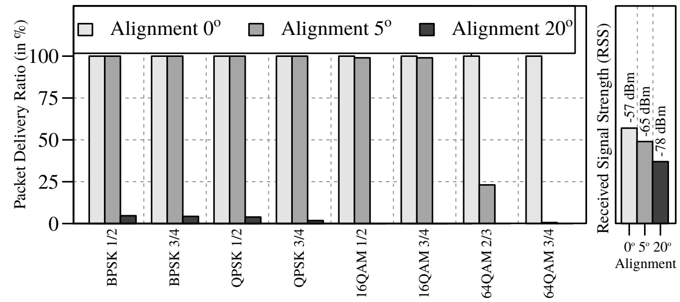

a) PDR for each MCS during daytime with different alignment angles at 40 m distance. b) RSS.

Figure 17. Impact of optic design misalignment on PDR and RSS.

G. Impact of Optics Misalignment

We also investigated the impact of optic design misalignment on the receiver's performance. Figure 17 shows the resulting PDRs and RSS due to optics misalignment at a distance of 40 m during day time. It can be seen that the PDR starts to drop sharply when the misalignment angle is increased from 0° to 20°, where the impact is much more drastic for higher order MCS. The figure also shows on the RSS. It can be noticed that with 20° of misalignment, the RSS is dropped down by 21 dB. These results clearly underline the criticality and possible human measurement errors involved in reproducing similar results over different iterations. At the same time, they also indicate the sensitivity of the receiver's performance on the optic design alignment. Possible solutions to reduce this sensitivity are to use optics with an optimized FoV or to use multiple photodiodes and spatial combining techniques [25], [30], [31] to improve the received RSS. For the time being, this is not in our scope and left to future work.

Regardless of the sensitivity on optics alignment, the presented V-VLC prototype performs extremely well. The results demonstrate the capability to communicate error-free (even in bright sunlight) for over 75 m with lower order MCS, and up to 40 m with higher order MCS. These very optimistic PDR results, particularly with lower order MCS, certainly highlights the potential of V-VLC as a complementary wireless set-up to support V2V communications, and, as a result, to offload traffic to V-VLC in case of RF spectrum congestion.

H. Spectral Efficiency

Figure 18 shows the achievable spectral efficiency with our V-VLC prototype over increasing distance between transmitter

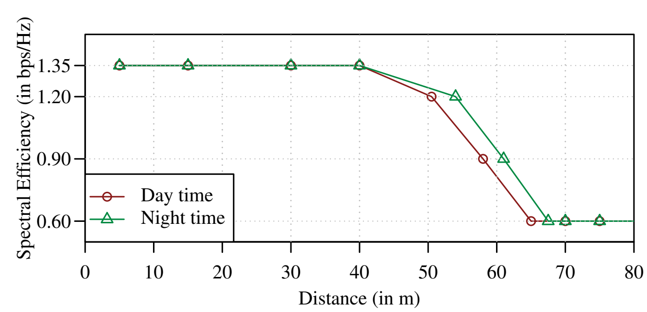

Figure 18. Achievable spectral efficiency over increasing distance.

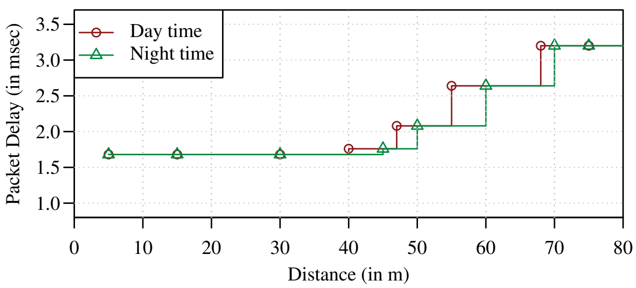

Figure 19. PLL for increasing distances between the transmitter and receiver.

and receiver at both day and night times. A maximum spectral efficiency of 1.35 bit/s/Hz is observed up to a distance of 40 m. With a 1 MHz sampling frequency, this translates to a bit rate of 1.35 Mbit/s. Likewise, the smallest observed spectral capacity is 0.6 bit/s/Hz, i.e., a bit rate of 600 kbit/s, with a sampling frequency of 1 MHz. As mentioned before, this 1 MHz sampling frequency limitation is only because of the low switching frequency of the LEDs in the used headlight and, quite certainly, with high switching frequency headlights, these bit rates can be improved by a great deal. Despite that, compared to the V-VLC literature (e.g., [22]), the prototype presented in this work, offers at least a 6-folds increase in the achievable bit rate in outdoor conditions, regardless of the time of the day.

I. Physical Layer Latency

Figure 19 shows the Physical Layer Latency (PLL), i.e., the time duration a payload engages as it transverses from the transmitter to the receiver. These results are obtained for a payload of size 250 B, which is sent over the channel with different MCS. It can be gathered from the figure that a minimum of about 1.7 ms duration is consumed by the payload for up to 40 m. Afterwards, the PLL increases sharply with further distances This higher PLL is due to the fact that a larger separation distance between the transmitter and receiver, results in lower Received Signal Strength, consequently, a lower order Modulation and Coding Schemes is used to ensure the correct decoding at the receiver. A lower order MCS requires more samples to send the same information as compared to a higher order MCS. Intuitively, more samples imply additional channel occupation for over-the-air transmissions, and as a result, we observed higher PLL at farther distances.

VI. Conclusion

We presented a complete system for experimental V-VLC research. All signal processing is done within the GNU Radio framework, which allows flexible rapid prototyping of complex signal processing in software. Our system supports OFDM with a variety of MCSs and is compliant to IEEE 802.11. On the sender side, our prototype is using a typical car lighting module for the front-end, which we connect to the used SDR by means of a custom driver electronics for the high power LEDs. On the receiver side, we rely on an off-the-shelf photodiode, which, again, is connected to an SDR. We show that this setup is already quite suitable for V-VLC-based communication between cars. We extended the prototype with rather simple optic design to focus the received modulated light and to block the ambient light. We performed an extensive outdoor measurement series to evaluate the performance of the system. As can be seen from the presented results, under perfect light conditions, we are able to reliably transmit with higher order MCS, for distances as large as 40 m Furthermore, during the day time, i.e., in strong sunlight, we are still able to keep the communication distances high but have to switch to lower order MCS in order to maintain the same low packet error rate and high reliability.

In conclusion, the presented prototype can easily be used for standard compliant V-VLC communication for typical outdoor driving scenarios. We anticipate a broad range of experiments in the field of cooperative automated driving, which can be performed on this basis. Given the flexibility of the used software and hardware components, the framework can easily be extended for further studies. Furthermore, by employing techniques such as Adaptive Modulation and Coding (AMC), where each OFDM subcarrier adopts an MCS dynamically based on its received SNR, the data rate per subcarrier can be optimized, which we believe will lead to an overall improved link capacity.

References

[1] D. Karunatilaka, F. Zafar, V. Kalavally, and R. Parthiban, “LED Based Indoor Visible Light Communications: State of the Art,” *IEEE Communications Surveys & Tutorials*, vol. 17, no. 3, pp. 1649–1678, Mar. 2015.

[2] P. H. Pathak, X. Feng, P. Hu, and P. Mohapatra, “Visible Light Communication, Networking, and Sensing: A Survey, Potential and Challenges,” *IEEE Communications Surveys & Tutorials*, vol. 17, no. 4, pp. 2047–2077, Feb. 2015.

[3] L. E. M. Matheus, A. B. Vieira, L. F. M. Vieira, M. A. M. Vieira, and O. Gnawali, “Visible Light Communication: Concepts, Applications and Challenges,” *IEEE Communications Surveys & Tutorials*, vol. 21, no. 4, pp. 3204–3237, 2019.

[4] S. Dimitrov and H. Haas, *Principles of LED Light Communications: Towards Networked Li-Fi*. Cambridge University Press, 2015.

[5] “IEEE Standard for Local and metropolitan area networks – Part 15.7: Short-Range Wireless Optical Communication Using Visible Light,” IEEE, Std 802.15.7-2011, Sep. 2011.

[6] A. Memedi and F. Dressler, “Vehicular Visible Light Communications: A Survey,” *IEEE Communications Surveys & Tutorials*, vol. 23, no. 1, pp. 161–181, Jan. 2021.

[7] A.-M. Cailean and M. Dimian, “Current Challenges for Visible Light Communications Usage in Vehicle Applications: A Survey,” *IEEE Communications Surveys & Tutorials*, vol. 4, no. 19, pp. 2681–2703, 2017.

[8] S.-H. Yu, O. Shih, H.-M. Tsai, N. Wisitpongphan, and R. Roberts, “Smart automotive lighting for vehicle safety,” *IEEE Communications Magazine (COMMAG)*, vol. 51, no. 12, pp. 50–59, Dec. 2013.

[9] C. B. Liu, B. Sadeghi, and E. W. Knightly, “Enabling Vehicular Visible Light Communication (V2LC) Networks,” in *8th ACM International Workshop on Vehicular Internetworking (VANET 2011)*, Las Vegas, NV: ACM, Sep. 2011, pp. 41–50.

[10] T. Yamazato, I. Takai, H. Okada, T. Fujii, T. Yendo, S. Arai, M. Andoh, T. Harada, K. Yasutomi, K. Kagawa, and S. Kawahito, “Image-Sensor-Based Visible Light Communication for Automotive Applications,” *IEEE Communications Magazine (COMMAG)*, vol. 52, no. 7, pp. 88–97, Jul. 2014.

[11] A. Memedi, H.-M. Tsai, and F. Dressler, “Impact of Realistic Light Radiation Pattern on Vehicular Visible Light Communication,” in *IEEE Global Communications Conference (GLOBECOM 2017)*, Singapore, Singapore: IEEE, Dec. 2017.

[12] M. S. Amjad, C. Tebruegge, A. Memedi, S. Kruse, C. Kress, C. Scheytt, and F. Dressler, "An IEEE 802.11 Compliant SDR-based System for Vehicular Visible Light Communications," in *IEEE International Conference on Communications (ICC 2019)*, Shanghai, China: IEEE, May 2019.

[13] M. Segata, R. Lo Cigno, H.-M. Tsai, and F. Dressler, "On Platooning Control using IEEE 802.11p in Conjunction with Visible Light Communications," in *12th IEEE/IFIP Conference on Wireless On demand Network Systems and Services (WONS 2016)*, Cortina d'Ampezzo, Italy: IEEE, Jan. 2016, pp. 124–127.

[14] M. Schettler, A. Memedi, and F. Dressler, "Deeply Integrating Visible Light and Radio Communication for Ultra-High Reliable Platooning," in *15th IEEE/IFIP Conference on Wireless On demand Network Systems and Services (WONS 2019)*, Wengen, Switzerland: IEEE, Jan. 2019, pp. 36–43.

[15] C. Tebruegge, A. Memedi, and F. Dressler, "Reduced Multiuser-Interference for Vehicular VLC using SDMA and Matrix Headlights," in *IEEE Global Communications Conference (GLOBECOM 2019)*, Waikoloa, HI: IEEE, Dec. 2019.

[16] S. Ucar, S. Coleri Ergen, and O. Ozkasap, "IEEE 802.11p and Visible Light Hybrid Communication based Secure Autonomous Platoon," *IEEE Transactions on Vehicular Technology (TVT)*, vol. 67, no. 9, pp. 8667–8681, Sep. 2018.

[17] B. Turan, G. Gurbilek, A. Uyrus, and S. Coleri Ergen, "Vehicular VLC Frequency Domain Channel Sounding and Characterization," in *10th IEEE Vehicular Networking Conference (VNC 2018)*, Taipei, Taiwan: IEEE, Dec. 2018.

[18] J. Koepe, C. Kaltschmidt, M. Illian, R. Puknat, P. Kneuper, S. Wittemeier, A. Memedi, C. Tebruegge, M. S. Amjad, S. Kruse, C. Kress, C. Scheytt, and F. Dressler, "First Performance Insights on Our Novel OFDM-based Vehicular VLC Prototype," in *10th IEEE Vehicular Networking Conference (VNC 2018), Poster Session*, Taipei, Taiwan: IEEE, Dec. 2018.

[19] O. Narmanlioglu, B. Turan, S. Coleri Ergen, and M. Uysal, "Cooperative MIMO-OFDM based inter-vehicular visible light communication using brake lights," *Elsevier Computer Communications*, vol. 120, no. C, pp. 138–146, May 2018.

[20] S. Kruse, C. Kress, A. Memedi, C. Tebruegge, M. S. Amjad, C. Scheytt, and F. Dressler, "Design of an Automotive Visible Light Communications Link using an Off-The-Shelf LED Headlight," in *16th GMM/ITG-Symposium ANALOG 2018*, Munich, Germany: VDE, Sep. 2018.

[21] W.-H. Shen and H.-M. Tsai, "Testing Vehicle-to-Vehicle Visible Light Communications in Real-World Driving Scenarios," in *9th IEEE Vehicular Networking Conference (VNC 2017)*, Turin, Italy: IEEE, Nov. 2017, pp. 187–194.

[22] B. Béchadergue, W.-H. Shen, and H.-M. Tsai, "Comparison of OFDM and OOK modulations for vehicle-to-vehicle visible light communication in real-world driving scenarios," *Elsevier Ad Hoc Networks*, vol. 94, Nov. 2019.

[23] B. Bloessl, M. Segata, C. Sommer, and F. Dressler, "An IEEE 802.11a/g/p OFDM Receiver for GNU Radio," in *ACM SIGCOMM 2013, 2nd ACM Software Radio Implementation Forum (SRIF 2013)*, Hong Kong, China: ACM, Aug. 2013, pp. 9–16.

[24] ——, "Performance Assessment of IEEE 802.11p with an Open Source SDR-based Prototype," *IEEE Transactions on Mobile Computing (TMC)*, vol. 17, no. 5, pp. 1162–1175, May 2018.

[25] C. Tebruegge, Q. Zhang, and F. Dressler, "Optical Interference Reduction with Spatial Filtering Receiver for Vehicular Visible Light Communication," in *IEEE International Conference on Intelligent Transportation Systems (ITSC 2019)*, Auckland, New Zealand: IEEE, Oct. 2019.

[26] A. Valberg, *Light Vision Color*. Wiley, 2007.

[27] L. Simonot and P. Boulenguez, "Generalization of the geometric description of a light beam in radiometry and photometry," *Journal of the Optical Society of America A (JOSA A)*, vol. 30, no. 4, pp. 589–595, Apr. 2013.

[28] Y. Wang, L. Tao, X. Huang, J. Shi, and N. Chi, "8-Gb/s RGBY LED-Based WDM VLC System Employing High-Order CAP Modulation and Hybrid Post Equalizer," *IEEE Photonics Journal*, vol. 7, no. 6, Oct. 2015.

[29] N. Kumar, N. Lourenço, D. Terra, L. N. Alves, and R. L. Aguiar, "Visible Light Communications in Intelligent Transportation Systems," in *IEEE Intelligent Vehicles Symposium (IV 2012)*, Alcalá de Henares, Spain: IEEE, Jun. 2012.

[30] A. Tsiatmas, F. M. J. Willems, and S. Baggen, "Optimum diversity combining techniques for visible light communication systems," in *IEEE Global Communications Conference (GLOBECOM 2014), 5th IEEE Workshop on Optical Wireless Communications (OWC 2014)*, Austin, TX: IEEE, Dec. 2014.

[31] M. Nabeel, B. Bloessl, and F. Dressler, "Efficient Receive Diversity in Distributed Sensor Networks using Selective Sample Forwarding," *IEEE Transactions on Green Communications and Networking (TGCN)*, vol. 2, no. 2, pp. 336–345, Jun. 2018.

Muhammad Sohaib Amjad (amjad@ccs-labs.org) is a Researcher/PhD student in the Telecommunication Networks Group (TKN) at TU Berlin. He received his MSc in electronics engineering from Sabanci University, Istanbul, Turkey in 2016, and his BSc in electrical engineering from Air University, Islamabad, Pakistan in 2011. His research focuses on topics related to wireless communications – physical layer signal processing, more specifically full-duplex wireless communication, mmWave communications, and vehicular visible light communication (V-VLC). He is an IEEE COMSOC student member and serves as a reviewer for manuscripts in the field of wireless communications.

Claas Tebruegge (tebruegge@ccs-labs.org) received his BSc in General Engineering Science (2014) and his MSc in Electrical Engineering (2016) at Hamburg University of Technology (TUHH). Afterwards he joined the Distributed Embedded Systems Group and working in cooperation with HELLA GmbH & Co. KGaA and the E-LAB towards his PhD. His reseach focuses on visible light-based vehicular communication. His focus is on the design of optics and electronics hardware for the implementation of prototypes, modulation and coding, signal processing, analytical studies as a basis for simulations, as well as system engineering. He is a student member of IEEE COMSOC and IEEE ITSS.

Agon Memedi (memedi@ccs-labs.org) is a Researcher/PhD student in the Telecommunication Networks Group (TKN) at TU Berlin. He received his M.Sc. in Computer Science from Paderborn University in 2015, and his B.Sc. in Computer Engineering from South East European University (SEEU) in 2011. His research focuses on the development of communication protocols and realistic simulation models for Vehicular Visible Light Communications (V-VLC). He is the author of Veins VLC, the V-VLC extension for the vehicular network simulation framework Veins. Agon has contributed in the organization of international conferences, such as IEEE VNC 2014, ACM MobiHoc 2016, and IEEE VNC 2019. Since September 2019, he is a Fulbright visiting scholar with the research group of Prof. Danijela Cabric in the Electrical and Computer Engineering Department at University of California, Los Angeles (UCLA).

Stephan Kruse (stkruse@hni.upb.de) received his B.S. and M.S. degrees in electrical engineering from the University of Paderborn, Paderborn, Germany, in 2015 and 2017, respectively. He is currently working toward the Ph.D. degree with the Heinz Nixdorf Institute, Paderborn, researching mm-Wave analog integrated circuits for wireless applications with silicon photonics technology. He has also investigated and developed novel transmission topologies for vehicular visible light communication.

Christian Kress (kressc@hni.upb.de) received the B.S. and M.S. degrees in electrical engineering from the University of Paderborn, Paderborn, Germany, in 2013 and 2017, respectively. He is currently working towards the Ph.D. degree with the Heinz Nixdorf Institute, Paderborn, researching high-frequency analog integrated circuits for broadband transmitters and receivers in silicon photonics technology.

J. Christoph Scheytt (cscheytt@hni.upb.de) received his diploma degree (M.Sc., 1996) and PhD degree (2000, with highest honors) both from Ruhr-University Bochum, Germany. In 2000 he co-founded advICo microelectronics GmbH, a German IC design house for RFIC and fiber-optic IC design. For 6 years he served as CEO at advICo. From 2006 to 2012 he was with IHP Leibnizinstitute for High-Performance Microelectronics in Frankfurt (Oder) as head of IHP's circuit design department. In 2012 Dr. Scheytt was appointed as full professor for Circuit Design by University of Paderborn, Germany and research group leader at the Heinz-Nixdorf Institute in Paderborn. From 2016 he served as chairman of the board of directors of the Heinz Nixdorf Institute. Since 2018 he is leader of the Priority Programme "Ultrafast Electronic-Photonics Integrated Systems for Ultrafast Signal Processing" SPP 2111) of the Deutsche Forschungsgemeinschaft. Dr. Scheytt has authored and co-authored more than 175 refereed journal papers and conference contributions and holds 15 patents. His research interests focus on high-frequency and broadband IC design for communications and sensing, IC design with SiGe BiCMOS and CMOS technologies, and silicon photonics.

Falko Dressler (dressler@ccs-labs.org) is full professor and Chair for Data Communications and Networking at the School of Electrical Engineering and Computer Science, TU Berlin. He received his M.Sc. and Ph.D. degrees from the Dept. of Computer Science, University of Erlangen in 1998 and 2003, respectively. Dr. Dressler has been associate editor-in-chief for IEEE Trans. on Mobile Computing and Elsevier Computer Communications as well as an editor for journals such as IEEE/ACM Trans. on Networking, IEEE Trans. on Network Science and Engineering, Elsevier Ad Hoc Networks, and Elsevier Nano Communication Networks. He has been chairing conferences such as IEEE INFOCOM, ACM MobiSys, ACM MobiHoc, IEEE VNC, IEEE GLOBECOM. He authored the textbooks Self-Organization in Sensor and Actor Networks published by Wiley & Sons and Vehicular Networking published by Cambridge University Press. He has been an IEEE Distinguished Lecturer as well as an ACM Distinguished Speaker. Dr. Dressler is an IEEE Fellow as well as an ACM Distinguished Member. He is a member of the German National Academy of Science and Engineering (acatech). He has been serving on the IEEE COMSOC Conference Council and the ACM SIGMOBILE Executive Committee. His research objectives include adaptive wireless networking (radio, visible light, molecular communications) and embedded system design (from microcontroller to Linux kernel) with applications in ad hoc and sensor networks, the Internet of Things, and cooperative autonomous driving systems.